The Astrophysical Journal, 634:L93–L96, 2005 November 20
© 2005. The American Astronomical Society. All rights reserved. Printed in U.S.A.

THE GROWTH, POLARIZATION, AND MOTION OF THE RADIO AFTERGLOW FROM THE GIANT FLARE FROM SGR 1806−20

G. B. Taylor,[1,2] J. D. Gelfand,[3] B. M. Gaensler,[3] J. Granot,[1] C. Kouveliotou,[4] R. P. Fender,[5] E. Ramirez-Ruiz,[6] D. Eichler,[7] Y. E. Lyubarsky,[7] M. Garrett,[8] and R. A. M. J. Wijers[9]

Received 2005 April 16; accepted 2005 July 27; published 2005 November 8

ABSTRACT

The extraordinary giant flare (GF) of 2004 December 27 from the soft gamma repeater SGR 1806−20 was followed by a bright radio afterglow. We present an analysis of VLA observations of this radio afterglow from SGR 1806−20, consisting of previously reported 8.5 GHz data covering days 7–20 after the GF, plus new observations at 8.5 and 22 GHz from day 24 to 81. We detect motion in the flux centroid of the afterglow, at an average velocity of $(0.26 \pm 0.03)c$ (assuming a distance of 15 kpc) at a position angle of −45°. This motion, in combination with the growth and polarization measurements, suggests an asymmetric outflow, mainly from one side of the magnetar. We find a deceleration in the expansion, from ∼9 to <5 mas day^{-1}. The time of deceleration is roughly coincident with the rebrightening in the radio light curve, as expected to result when the ejecta from the GF sweeps up enough of the external medium and transitions from a coasting phase to the Sedov-Taylor regime. The radio afterglow is elongated and maintains a 2 : 1 axis ratio with an average position angle of −40° (north through east), oriented perpendicular to the average intrinsic linear polarization angle.

Subject headings: pulsars: individual (SGR 1806−20) — radio continuum: general — stars: flare — stars: neutron — stars: winds, outflows

1. INTRODUCTION

The spectacular giant flare (GF) of 2004 December 27 from the soft gamma repeater SGR 1806−20 is believed to have originated from a violent magnetic reconnection event in this magnetar (Palmer et al. 2005; Hurley et al. 2005). This sudden energy release of more than 10^{46} ergs in gamma rays (assuming isotropic emission at a distance of 15 kpc; Corbel & Eikenberry 2004; McClure-Griffiths & Gaensler 2005) managed to eject a significant amount of baryons, probably accompanied by some pairs and magnetic fields, from the neutron star (Palmer et al. 2005; Gelfand et al. 2005; Granot et al. 2005). As this outflow interacted with the external medium, it powered an expanding radio afterglow (Cameron & Kulkarni 2005; Gaensler et al. 2005) at least 500 times more luminous than the only other radio afterglow detected from an SGR GF (Frail et al. 1999). After a steep decay ($\sim t^{-2.7}$; Gaensler et al. 2005), a rebrightening in the radio light curve was seen, starting at $t \sim 25$ days and peaking at $t \sim 33$ days (Gelfand et al. 2005), followed by a shallower decay. This is most naturally explained by the transition from free expansion to the Sedov-Taylor phase, which occurs when a sufficient mass of ambient medium is swept up (Gelfand et al. 2005; Granot et al. 2005).

[1] Kavli Institute of Particle Astrophysics and Cosmology, Menlo Park, CA 94025.

[2] National Radio Astronomy Observatory, P.O. Box O, 1003 Lopezville Road, Socorro, NM 87801.

[3] Harvard-Smithsonian Center for Astrophysics, 60 Garden Street, Cambridge, MA 02138.

[4] NASA Marshall Space Flight Center, XD-12, NSSTC, 320 Sparkman Drive, Huntsville, AL 35805.

[5] School of Physics and Astronomy, University of Southampton, Highfield, Southampton SO17 1BJ, UK.

[6] Institute for Advanced Study, Einstein Drive, Princeton, NJ 08540.

[7] Department of Physics, Ben-Gurion University, P.O. Box 653, Beér Sheva 84105, Israel.

[8] Joint Institute for VLBI in Europe, Postbus 2, 7990 AA, Dwingeloo, Netherlands.

[9] Astronomical Institute "Anton Pannekoek," University of Amsterdam, Kruislaan 403, 1098 SJ, Amsterdam, Netherlands.

2. OBSERVATIONS

The NRAO[10] Very Large Array (VLA) observations of SGR 1806−20 began 6.9 days after the GF with the VLA in its A configuration. Here we report all 8.5 and 22 GHz observations up through day 81 (see Table 1). The first 20 days of monitoring with a host of radio telescopes including the VLA have previously been described by Gaensler et al. (2005) and by Cameron et al. (2005). Absolute flux calibration was obtained from a short observation of 3C 286 during each run. Phase calibration was determined by observations of the strong (0.75 Jy) but somewhat distant (5.°78) calibrator PMN J1820−2528 or (from 2005 January 16 on) the nearby (0.°77) and moderately strong (0.32 Jy) calibrator TXS J1811−2055 with a cycle time of 3.5 minutes. From January 16 onward, the validity of the phase transfer at 8.5 GHz was checked by short observations of J1820−2528 every 15 minutes. In general, the coherence was found to be better than 95% on J1820−2528. For all observations except those on 2005 January 3, the strong and unpolarized source OQ 208 was observed for 1 minute in order to permit solving for the instrumental polarization. For the data on January 3, leakage terms were transferred from observations of BL Lac on 2005 January 2. The absolute polarization angle was referenced to 3C 286 for all epochs.

3. MODEL FITTING AND ERROR ANALYSIS

In all observations reported here, the radio afterglow of SGR 1806−20 is smaller than the naturally weighted synthesized beam. Since the signal-to-noise ratio is high, however, it is quite feasible to extract information about the size and shape of the source by fitting models to the visibility data. For each of the epochs, we fit a two-component model to the data for the SGR 1806−20 field. One elliptical, two-dimensional Gaussian component (with the six free parameters given in Table 2) describes

[10] The National Radio Astronomy Observatory is operated by Associated Universities, Inc., under cooperative agreement with the National Science Foundation.

TABLE 1
OBSERVATIONAL SUMMARY

Date	t (days)	Freq. (GHz)	Phase Calibrator	Time (minutes)	rms noise (μJy beam^{-1})	Array Config.	$B_{\rm min}$ (mas)	$B_{\rm maj}$ (mas)	$B_{\rm P.A.}$ (deg)
2005 Jan 3	6.9	8.5	J1820−2528	12	60	A	222	458	16
2005 Jan 5	8.8	8.5	J1820−2528	15	70	A	213	542	−27
2005 Jan 6	9.9	8.5	J1820−2528	34	34	A	233	430	19
2005 Jan 7	11.0	8.5	J1820−2528	18	61	A	233	717	41
2005 Jan 10	13.7	8.5	J1751−2524	26	45	A	228	811	−41
2005 Jan 13	16.8	8.5	J1820−2528	38	25	A	295	597	29
2005 Jan 16	19.9	8.5	J1811−2055	28	31	A	408	605	−42
2005 Jan 20	23.8	22.5	J1811−2055	37	59	BnA	190	317	−75
2005 Jan 24	27.7	8.5	J1811−2055	21	30	BnA	451	1004	−60
2005 Jan 27	30.7	8.5	J1811−2055	32	36	BnA	382	1346	53
2005 Feb 3	37.7	8.5	J1811−2055	21	40	BnA	437	1062	−60
2005 Feb 7	41.7	8.5	J1811−2055	21	…	BnA	…	…	…
2005 Feb 11	45.7	8.5	J1811−2055	17	40	BnA	401	1328	−55
2005 Feb 20	54.7	8.5	J1811−2055	111	15	B	736	1323	−14
2005 Feb 26	60.7	8.5	J1811−2055	17	48	B	706	1465	−22
2005 Mar 4	66.7	8.5	J1811−2055	66	36	B	720	1296	3
2005 Mar 12	74.7	8.5	J1811−2055	26	42	B	730	1305	3
2005 Mar 19	81.7	8.5	J1811−2055	37	44	B	736	1351	14

NOTES.—VLA data from February 7 were unusable due to poor observing conditions. February 11 includes data taken on February 10 and 12. February 20 includes data taken on February 19 and 21. The second column gives t, the time after the GF; the fifth column refers to the total integration time on-source; and $B_{\rm maj}$, $B_{\rm min}$, and $B_{\rm P.A.}$ describe the naturally weighted synthesized restoring beam measured north through east.

SGR 1806−20, while a point source (not listed) was used to describe the radio nebula associated with the luminous blue variable star approximately 14″ to the east (Frail et al. 1997). Other models for the radio afterglow, including an elliptical ring, a uniform sphere, an elliptical disk, and two point sources, were tried but were not found to provide a better fit. Fitting the VLA data to an elliptical ring or disk at any epoch increases the derived size by a factor of ∼1.16 or ∼1.66, respectively, as expected (Pearson 1999). The model fitting was performed in both MIRIAD (task UVFIT) and Difmap and was found to agree to within the uncertainties. We adopt the MIRIAD fits (Table 2) and the estimated statistical errors. As in Taylor et al. (2004), the error of the size was checked with Monte Carlo simulations of the data using identical (u, v)-coverage, similar noise properties, and a Gaussian component of known size added. The simulations confirm the error estimates quoted by MIRIAD and agree with errors estimated from the signal-to-noise ratio and the synthesized beam shape.

In the early epochs, there is some evidence from the MERLIN and VLBA observations (Fender et al. 2005) that the morphology of the source is more complicated than an elliptical Gaussian and may experience rapid changes in the location of the peak emission. These changes in the surface brightness could cause shifts in the centroid of our model fits and deviations in the fitted size. For this reason, we have added a 10% error in quadrature to the measured size of all points, although

TABLE 2
MODEL FITTING AND POLARIMETRY RESULTS

t (days)	Flux (mJy)	Δx (mas)	Δy (mas)	θ_M (mas)	Axial Ratio	$\theta_{\rm P.A.}$ (deg)	Pol. (%)	ϕ (deg)
6.9	54.59 ± 0.09	…	…	79.4 ± 0.9	0.52 ± 0.06	−58 ± 2	2.1 ± 0.1	20 ± 2
8.8	32.30 ± 0.09	0	0	67.8 ± 4.9	0.50 ± 0.12	−65 ± 8	1.3 ± 0.2	12 ± 2
9.9	23.68 ± 0.04	28	2	78.6 ± 1.2	0.55 ± 0.06	−52 ± 3	1.1 ± 0.1	4 ± 4
11.0	16.78 ± 0.06	47	−5	85.8 ± 2.4	0.68 ± 0.03	−68 ± 12	1.6 ± 0.3	12 ± 5
13.7	9.75 ± 0.05	…	…	120.3 ± 16.3	0.70 ± 0.10	−59 ± 12	1.9 ± 0.3	44 ± 6
16.8	5.65 ± 0.04	37	−9	121.6 ± 5.9	0.80 ± 0.13	−87 ± 24	2.6 ± 0.3	38 ± 5
19.9	4.18 ± 0.05	10	26	197.7 ± 12.8	0.54 ± 0.08	−54 ± 8	3.4 ± 0.5	35 ± 12
23.8	1.62 ± 0.12	−19	56	208.9 ± 40.7	0.84 ± 0.25	−31 ± 46	…	…
27.7	3.24 ± 0.06	−36	71	276.1 ± 42.3	0.65 ± 0.12	−44 ± 11	<2.0	…
30.7	3.93 ± 0.06	−68	111	292.3 ± 17.7	0.82 ± 0.22	−26 ± 31	<2.2	…
37.7	3.22 ± 0.06	−70	91	258.3 ± 37.5	0.43 ± 0.26	−15 ± 16	<2.4	…
45.7	2.60 ± 0.05	−61	97	346.4 ± 38.9	0.59 ± 0.11	−26 ± 10	<5.7	…
54.7	2.03 ± 0.03	−78	109	352.5 ± 41.7	0.73 ± 0.10	−21 ± 11	<1.5	…
60.7	1.78 ± 0.07	−67	75	461.4 ± 117	0.60 ± 0.30	−28 ± 17	<4.7	…
65.7	1.72 ± 0.04	−92	107	446.8 ± 50.6	0.53 ± 0.09	−12 ± 7	<2.6	…
74.7	1.55 ± 0.06	−113	128	446.1 ± 90.3	0.56 ± 0.16	−11 ± 13	<3.9	…
81.7	1.39 ± 0.05	−135	141	459.1 ± 78.6	0.49 ± 0.22	−23 ± 15	<4.4	…

NOTES.—Positions are relative to that derived on January 5, which is R.A. = $18^{\rm h}08^{\rm m}39\overset{\rm s}{.}3418$, decl. = $-20°24'39\overset{''}{.}827$ (J2000). The positions of January 3 and 10 are excluded for reasons described in the text. The errors quoted on the flux densities are only statistical and will be discussed in a future paper. Position errors are dominated by an ∼20 mas systematic uncertainty in the astrometry. The source size is described by the major axis θ_M, axial ratio, and position angle $\theta_{\rm P.A.}$. Note that the position angle at 13.7 days after the burst differs substantially from the value of 62° ± 14° shown in Fig. 3 of Gaensler et al. (2005). The new fit presented here seems more consistent with the position angles seen at adjacent epochs. A subsequent paper will fully investigate this possible discrepancy. The source polarization is described by the fractional polarization and the electric vector polarization angle ϕ, where ϕ has been corrected for the observed rotation measure of 272 ± 10 rad m^{-2} (Gaensler et al. 2005).

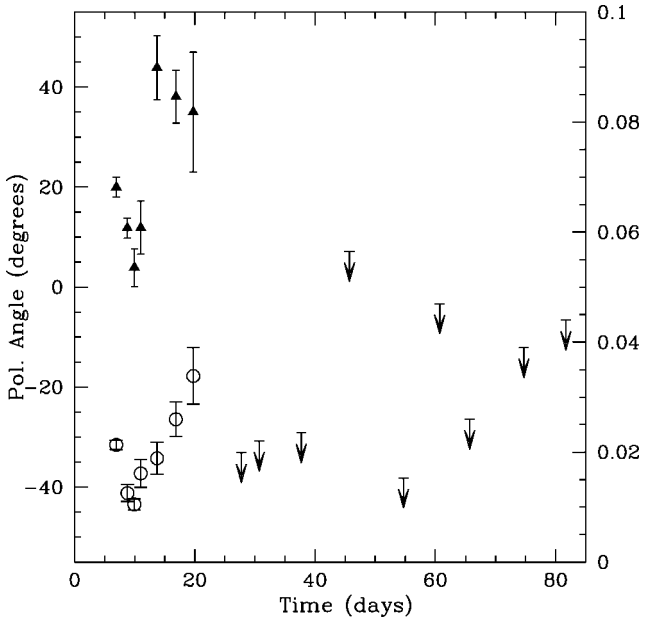

FIG. 1.—Linear fractional polarization (*circles*; right *y*-axis) and polarization angles (*triangles*; left *y*-axis) for the radio afterglow from SGR 1806−20 as a function of time at 8.5 GHz. All polarization angles have been corrected for the observed rotation measure of 272 ± 10 rad m^{-2} (Gaensler et al. 2005). Limits on fractional polarization are drawn at 3 σ.

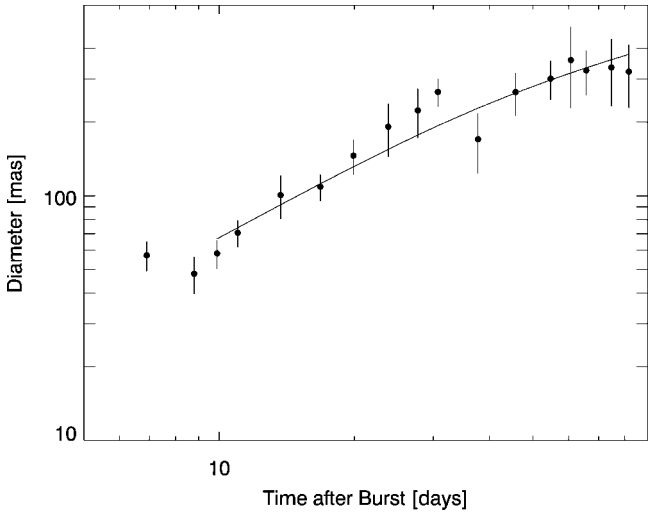

FIG. 2.—Expansion of the radio afterglow from SGR 1806−20 as a function of time. The size shown is the geometric mean of the major and minor axes of the best-fitting elliptical Gaussian for each observation. The solid line is a fit of a supersonically expanding shell model as described by eq. (4) of Gelfand et al. (2005). This model does not take into account the collimation and proper motion of the source, but provided that these are not extreme, it illustrates the deceleration due to mass loading by the external medium.

the error may be larger in the earlier measurements. At later times, 1.4 GHz MERLIN observations seem to be more consistent with a smooth elliptical Gaussian.

4. POLARIZATION, EXPANSION, AND PROPER MOTION

Linear polarization from the radio afterglow was detected during the first 20 days after the GF at 8.5 GHz (Gaensler et al. 2005). Thereafter we were only able to measure upper limits on the polarization (Fig. 1). The polarization is found to be 2.1% on day 7 and to decrease to a minimum of 1.1% on day 10. At that time, the linear polarization began to increase steadily to a maximum value of 3.4% while the polarization angle swung rapidly from 4° to 40°. The polarization falls below our detection limit of 2% around the time of the rebrightening in the light curve. Limits as late as 55 days after the GF are below 2%.

In Figure 2 we plot the geometric mean diameter of the elliptical Gaussian model fits. These fits show the expansion of the radio afterglow from SGR 1806−20 over the first 81 days after the GF. As reported in Gaensler et al. (2005), SGR 1806−20 was clearly resolved in the earliest VLA observations taken 7 days after the GF with a diameter of ~57 mas (mean full width). MERLIN observations (Fender et al. 2005) reveal that the source could be asymmetric. The size and position angle of the MERLIN extension at −31° is roughly consistent with our average value of −40 ± 20. There is some possible evidence for a gradual swing in the position angle of the VLA data (Table 2), and we will investigate its significance in a future paper. Assuming a one-sided expansion (as argued in § 5), the apparent velocity required to reach a size of 57 mas in 6.9 days is 8.3 ± 0.9 mas day^{-1} [$(0.72 \pm 0.10)d_{15}c$)].

After 30 days (the time of the rebrightening reported by Gelfand et al. 2005), the radio afterglow had grown to ~260 mas (full width of the geometric mean of the major and minor axes). Between 7 and 30 days, the growth of the radio nebula from 57 to 260 mas corresponds to an average expansion velocity of 9.0 ± 1.6 mas day^{-1} [$(0.78 \pm 0.14)d_{15}c$]. After this time, the growth appears to slow so that the average velocity between day 30 and the last day of observations reported here is 1.0 ± 2 mas day^{-1} ($<0.4d_{15}c$), where the source size reaches ~322 mas. This expansion is in agreement with the MERLIN size estimate of ~390 mas (mean full width), 56 days after the GF.

Following Gelfand et al. (2005; see their eq. [4]), we fit to the data from day 9 onward a supersonically expanding spherical shell that is decelerated as it sweeps up material. While the deceleration of an anisotropic outflow might be somewhat different than in the spherical case, the latter may still serve as a rough approximation. The fit (reduced χ^2 of 0.76; shown as the solid line in Fig. 2) implies a deceleration time of 40 ± 13 days after the GF, consistent with the time of the peak rebrightening at day ~30 and the deceleration time of ~46 days derived from the rebrightening (Gelfand et al. 2005). We also fit a constant expansion (5.6 ± 0.6 mas day^{-1}) to the data and obtain a reduced χ^2 of 1.22. An *F*-test gives a probability of 2% that the constant expansion is an equally valid description of the data. A broken power law actually fits much better than either model (reduced $\chi^2 = 0.06$) but requires both acceleration and deceleration of the explosion.

Good astrometry was obtained for the radio afterglow from SGR 1806−20 on all days of the observations except 2005 January 3, January 10, and February 7 via phase referencing to a nearby calibrator. A combination of a long cycle time (15 minutes), distant calibrator (J1820−2528), and poor atmospheric phase stability resulted in a large systematic position error on January 3, although changes in the relative brightness of different parts of the image (Fender et al. 2005) may also have affected the centroid position. On January 10, the low elevation of the observations forced us to employ a distant calibrator with a poor position. On February 7, poor weather caused unstable phase conditions such that the coherence estimated on J1820−2528 was only 36%.

The centroid of the radio afterglow from SGR 1806−20 is found to shift by ~200 mas over the course of 70 days of observations (Fig. 3). We have decomposed this shift into *x*- and *y*-components (Table 2) and performed least-squares fits to the motion. The radial proper motion is 3.0 ± 0.34 mas

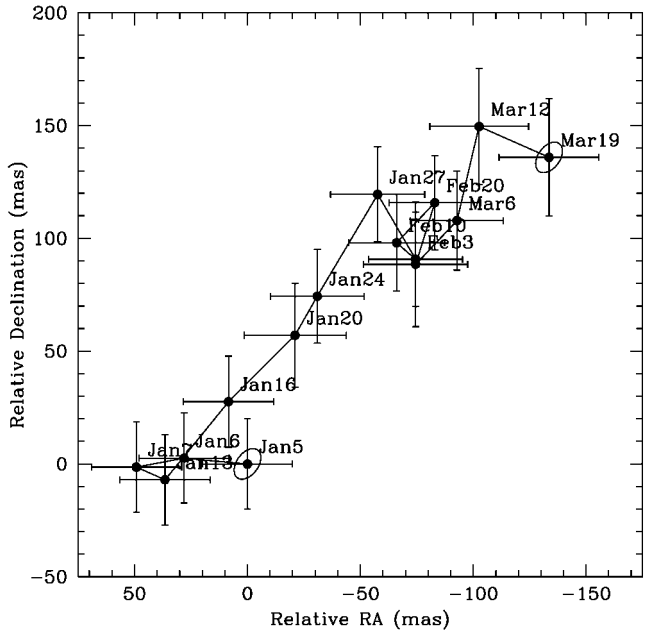

FIG. 3.—Trajectory of the afterglow of SGR 1806−20. Dates are labeled. The small ellipses denote the first and last days used.

day^{-1} at a position angle of $-44° \pm 6°$ (measured north through east). This motion corresponds to $(0.26 \pm 0.03)d_{15}c$. There is some indication that the time of fastest proper motion also corresponds to the time of fastest growth.

5. DISCUSSION

The motion of the radio flux centroid is along the major axis of the source and is roughly half of the growth rate. This may be naturally explained by a predominantly one-sided outflow, which produces a radio nebula extending from the location of the magnetar out to an increasing distance in the direction of the ejection. This suggests that either the catastrophic reconfiguration of the magnetic field that caused the GF was relatively localized, rather than a global event involving the whole magnetar (see Eichler 2002), or the baryonic content of the ejecta is asymmetric. It is also possible that the environment plays a role in collimating the outflow.

The position angle of the linear polarization is roughly perpendicular to the major axis of the image and to the direction of motion of the flux centroid. This naturally arises for a shock-produced magnetic field, which is tangled predominantly within the plane of the shock (Medvedev & Loeb 1999), because of the elongated shape of the emitting region and due to projection effects (Gaensler et al. 2005). Alternatively, this might be caused by shearing motion along the sides of the one-sided outflow, which can stretch the magnetic field in the emitting region along its direction of motion. The degree of polarization decreased at about the same time as the deceleration and rebrightening in the light curve (see Fig. 1). As the rebrightening is attributed to the emission from the shocked external medium becoming dominant (Gelfand et al. 2005; Granot et al. 2005), this suggests a lower polarization of this emission component. This, in turn, suggests that the magnetic field in the shocked interstellar medium (ISM) is less ordered than in the shocked ejecta and/or shocked external shell.

In the first 30 days, the outer edge of the radio afterglow moves away from the magnetar position at an apparent velocity of $0.8c$. The intrinsic velocity could be lower depending on the unknown inclination of the outflow. The minimum velocity is $0.62c$ for an angle of the outflow with a line of sight of 51°. This is in agreement with the high escape velocity of $0.5c$ for a neutron star. At these transrelativistic velocities (Lorentz factor 1.3), there is a modest increase in the total kinetic energy of the outflow. Compared to previous estimates based on isotropic outflows (Gelfand et al. 2005), the energy is increased by a factor of 2–3 owing to the factor of 2 higher velocity at the outer edge, but lower velocities elsewhere (Granot et al. 2005). Combining these two factors leads to a revised estimate for the total kinetic energy in the ejecta of $\sim 10^{45}$ ergs. By momentum conservation, a one-sided outflow of $10^{24.5}$ g (Granot et al. 2005) at $0.62c$ imparts a kick to the magnetar of 30 cm s^{-1}.

6. CONCLUSIONS

We report a deceleration in the observed expansion of the radio afterglow produced by the 2004 December 27 giant flare from SGR 1806−20. We also find a proper motion for the radio afterglow roughly aligned with its major axis and perpendicular to the average polarization angle. These observations support the idea of an asymmetric explosion on one side of the magnetar. The polarization data place significant constraints on the magnetic field structure in the shocked ejecta and ISM. Measurements with the VLA continue and will be presented in a future paper.

We thank an anonymous referee for constructive comments. J. D. G. and B. M. G. acknowledge the support of NASA through LTSA grant NAG5-13032. J. G. acknowledges support from the US Department of Energy under contract DE-AC03-76SF00515. D. E. acknowledges support from the Israel-US BSF, the ISF, and the Arnow Chair of Physics. Y. E. L. acknowledges support from the German-Israeli Foundation. E. R.-R is sponsored by NASA through *Chandra* Postdoctoral Fellowship award PF3-40028. R. A. M. J. W acknowledges support from the NWO.

REFERENCES

Cameron, P. B., & Kulkarni, S. R. 2005, GCN Circ. 2928
Cameron, P. B., et al. 2005, Nature, 434, 1112
Corbel, S., & Eikenberry, S. S. 2004, A&A, 419, 191
Eichler, D. 2002, MNRAS, 335, 883
Fender, R. P., et al. 2005, MNRAS, submitted
Frail, D. A., Kulkarni, S. R., & Bloom, J. S. 1999, Nature, 398, 127
Frail, D. A., Vasisht, G., & Kulkarni, S. R. 1997, ApJ, 480, L129
Gaensler, B. M., et al. 2005, Nature, 434, 1104
Gelfand, J. D., et al. 2005, ApJ, 634, L89
Granot, J., et al. 2005, ApJ, in press (astro-ph/0503251)
Hurley, K., et al. 2005, Nature, 434, 1098
McClure-Griffiths, N. M., & Gaensler, B. M. 2005, ApJ, 630, L161
Medvedev, M. V., & Loeb, A. 1999, ApJ, 526, 697
Palmer, D. M., et al. 2005, Nature, 434, 1107
Pearson, T. J. 1999, in ASP Conf. Ser. 180, Synthesis Imaging in Radio Astronomy II, ed. G. B. Taylor, C. L. Carilli, & R. A. Perley (San Francisco: ASP), 335
Taylor, G. B., Frail, D. A., Berger, E., & Kulkarni, S. R. 2004, ApJ, 609, L1